

# **Nanoscopic Carbon Electrodes: Structure, Electric Properties and Application for Electrochemistry**

Eser Metin Akinoglu<sup>1,2,3,\*</sup>, Enno Kätelhön<sup>4</sup>, Jonas Pampel<sup>3</sup>, Zhiyong Ban<sup>4</sup>, Markus Antonietti<sup>3</sup>, Richard G. Compton<sup>4</sup>, Michael Giersig<sup>1,2,\*</sup>

<sup>1</sup> *South China Normal University, International Academy of Optoelectronics at Zhaoqing, China*

<sup>2</sup> *Department of Physics, Freie Universität Berlin, Arnimalle 14, 14195 Berlin, Germany*

<sup>3</sup> *Max Planck Institute of Colloids and Interfaces, Am Mühlenberg 1, 14476 Potsdam, Germany,*

<sup>4</sup> *Department of Chemistry, Physical and Theoretical Chemistry Laboratory, Oxford University, South Parks Road, Oxford OX1 3QZ, United Kingdom*

*\*Corresponding Authors:*

*Eser M Akinoglu (e.a@fu-berlin.de ; Tel.: +49307121475)*

*Michael Giersig (giersig@physik.fu-berlin.de ; Tel.: +493083863172)*

## Abstract

For many electrochemical applications, glassy carbon is an important electrode material that acts as a catalyst support and carbon nanotubes are frequently exploited as a catalyst itself or as a support for other active materials. Here we demonstrate a carbon-based, nanostructured, and high surface area electrode that consist of individual, free standing and vertically aligned multi-wall carbon nanotubes (MWCNTs) directly grown on glassy carbon via direct current plasma enhanced chemical vapour deposition. The structure is characterized via electron microscopy techniques, and local current-voltage measurements on individual MWCNTs confirm a good Ohmic contact of the individual vertically aligned MWCNTs and the glassy carbon bulk electrode. The proposed electrode can be used as a model system to study the mass transport of vertically aligned one-dimensional nanomaterials in electrochemistry applications. Its electrochemical characteristics are investigated using aqueous  $\text{Ru}(\text{NH}_3)_6^{3+/2+}$  as an outer sphere redox couple. Cyclic voltammetry measurements show a significant increase in double-layer capacitance of the textured electrodes with respect to pristine glassy carbon. Finally, we demonstrate that the morphology of textured electrodes results in altered mass transport properties and yields a mixed linear- and thin-layer diffusion response depending on the scan rate, which is illustrated through numerical simulations.

## 1. Introduction

Carbon materials are widely used in analytical and industrial electrochemistry due to their wide potential window, relatively inert electrochemistry, and electrocatalytic activity in a variety of redox reactions.[1, 2] Different allotropes of carbon exhibit different electrochemical properties where glassy carbon (GC) is an electrochemically important variant of graphitic carbon which is widely used as an electrode that often serves as a catalyst supports.[1, 2] Another form of carbon are carbon nanotubes that consist of rolled up graphene layers with conductivity, density of electronic states and very high surface area, and are of particular interest in the context of energy storage, electroanalysis, electrocatalysis and as catalyst support.[1, 3, 4] The electrical properties of glassy carbon and MWCNTs have been extensively investigated and show a high electrical conductivity.[5] In this context, metallic conductivity has been reported in case of bamboo-shaped MWCNTs.[6] Further, Li *et al.* demonstrated that single MWCNTs have large current-carrying capacities and observed quasi-ballistic conducting behavior.[7] Consequently, MWCNTs are excellent candidates as single nanoscopic electrodes or as nanoscopic elements of a macroscopic electrode, both of which have promising electrochemical applications such as in electrocatalysis[8], electroanalysis[9–11] and energy storage[12, 13].[14, 15] Randomly oriented MWCNTs applied from solution and fixed with a binder onto a support electrode are expected to exhibit contact resistance problems and difficulty of conformal coating with a catalyst material. Hence it is desirable to obtain aligned MWCNT electrodes where each individual MWCNT is in direct electrical contact with its support material. One approach towards this goal is the alignment of functionalized CNTs. Shown for aligned CNT forests on gold electrodes via thiol groups,[9, 10] and on GC electrodes via amide bonds.[11] However, in these cases the electrical contact of the aligned CNTs is solely mediated by functional groups. Wang *et al.* demonstrated that CNT forests can be transferred on top of GC substrates and fixed with a binder.[16] A better approach is the direct growth of MWCNTs on a bulk electrode, which ideally is carbon based to insure mechanical stability.[17] Though, unaligned CNTs have

been grown directly on carbon fibres and graphite foils via CVD,[18, 19] vertically aligned CNTs directly grown on GC for their use in electrochemistry are a more interesting system. Park *et al.* showed that WMCNT *bundles* can be directly grown on GC electrodes via radio frequency plasma enhanced chemical vapour deposition (RF-PECVD) to obtain three dimensional micro electrodes.[17] In this article, we introduce a three dimensional carbon based macroelectrode with nanoscopic architecture. Vertically aligned and spaced out MWCNTs are directly grown on GC via direct current (DC) PECVD ensuring good electrical contact for each MWCNT. Voids of the several tens to hundreds of nanometers enable access of each MWCNT for potential catalyst deposition to create vertically aligned core-sheath nanowire arrays where each individual nanowire core has low intrinsic resistance as well as low contact resistance to the bulk electrode. The structure of the proposed backbone electrodes is characterized via electron microscopy whereas conductive atomic force microscopy (c-AFM) is used to probe the electrical properties of individual vertically aligned MWCNTs on the bulk GC surface. The electrode kinetics of MWCNT textured and pristine GC electrodes are compared for the case of the outer-sphere redox couple  $\text{Ru}(\text{NH}_3)_6^{3+/2+}$  which is insensitive to most surface defects and impurities,[20] and serves as a useful benchmark for electrode kinetics studies.[1] Their diffusion response is additionally explored through numerical studies through which we gain a deeper understanding of the electrochemical response of vertically aligned arrays of one dimensional nanomaterials. In particular the interplay of the role of (i) the active area defined by the nanostructured surface area (sides and tops) of the MWCNTs together with the exposed part of the supporting GC base with that of (ii) the macroscopic geometric area of the ensemble as a whole assuming a planar surface, is characterised and shown to be highly sensitive to the voltage scan rate used voltammetrically, or frequency employed in impedance spectroscopy. Specifically, in the limit of very slow scan rates or frequencies the response of the entire nanostructure simply reflects semi-infinite diffusion to the macroscopic geometric area of the entire structure whereas at faster scan rates or frequencies the actual surface area of the

MWCNT array becomes apparent as the response increasingly reflects a contribution from *thin layer* diffusion of material trapped within the solution filled voids between the MWCNTs.

## **2. Experimental**

### ***2.1 MWCNT Synthesis***

Vertically aligned MWCNTs were synthesized via the direct PECVD technique.[21, 22] First, polished glassy carbon discs of 1 mm thickness and 8 mm diameter purchased from HTW Hochtemperatur-Werkstoffe GmbH were coated with a 10 nm nickel film via electron beam evaporation. MWCNT growth was performed in a home built PECVD system at 750°C, where acetylene (C<sub>2</sub>H<sub>2</sub>) is used as the carbon source and ammonia (NH<sub>3</sub>) as the carrier gas with a ratio of 1:8 at a pressure of 6 mbar. The plasma power was maintained constant at 20 W.

### ***2.2 Measurement and Sample Characterization***

Scanning electron microscopy and transmission electron microscopy were performed using a Carl Zeiss LEO Gemini 1530 and a Philips CM12 respectively. EDX analysis was performed with a Thermo Scientific UltraDry EDS x-ray detector and NSS Spectral Analysis System at the SEM. Conductive atomic force microscopy was performed using a NTEGRA Prima model microscope by NT-MDT Co. employing silicon cantilevers coated with a 20-30 nm thick Au layer and a tip curvature of <30 nm. First, a topography image was collected in non-contact mode. Subsequently, the tip was approached onto a predefined location on the surface determined from the topography image where current-voltage (IV) curves were collected upon contact. The observed drift during the timescale of a single IV curve measurement were negligible. To compensate drift over larger time scales, a new topography image for each approached topography point was obtained. To increase the sensitivity of the measurement, a voltage divider was used to reduce the minimum output voltage of the instrument. Electrochemical measurements were conducted with a three-electrode set up in freshly prepared 1.0 M KCl solution using a Reference 600 potentiostat (Gamry Instruments). A home-made PTFE cell was used which enables the direct analysis of the pristine and MWCNT textured

glassy carbon discs, with a spherically exposed area of 0.7 mm in diameter. A graphite rod (diameter, 6 mm) and Ag/AgCl were used as counter and reference electrode, respectively. All the potentials were corrected to the internal resistance determined by impedance measurements at high frequencies. Prior to the measurements, the electrolyte was bubbled with nitrogen to remove oxygen from the solution. First, the CV-response in 1.0 M KCl was recorded between -0.5 and 0.3 V (vs. Ag/AgCl<sub>sat</sub>) applying different scan rates (10 to 500 mV/s). The kinetic studies were conducted under the same conditions but the electrolyte contained Ru(NH<sub>3</sub>)<sub>6</sub>Cl<sub>2</sub> (Sigma-Aldrich Co.) with a concentration of 1.0 mM.

### ***2.3 Simulations***

Simulations of the Faradaic response of textured electrodes were carried out using a previously-described software by Ban et al.,[23] which was only slightly modified and is similar to software used in related publications.[24, 25] In short, we modelled reversible voltammetry at ideally cylindrical electrodes that are vertically aligned on an insulating surface and patterned in a hexagonal fashion. The electrode ensemble as a whole was assumed to resemble a macro electrode, hence enabling the negligence of edge effects when diffusive mass transport is considered.[26]

The geometrical dimensions required for our calculations were extracted from SEM measurements via the image analysis software ImageJ. A mean height of  $h = 4 \mu\text{m}$  and a mean diameter of  $d = 98 \text{ nm}$  were found for the size of the nanopillars, and a mean pillar-to-pillar distance (edge-to-edge) of  $s = 222 \text{ nm}$  was measured assuming a hexagonal pattern of the pillars. On the basis of previous reports aiming at the determination of exact values in various electrolytes, we approximate the diffusion coefficient of both Hexaammineruthenium(II) and Hexaammineruthenium(III) to  $D = 6.6 \times 10^{-9} \text{ m}^2\text{s}^{-1}$ . [27]

We further note that our simulation made use of the diffusion domain approximation,[26, 28–31] which reduces the computational workload significantly. To this end, we did not model the

full array but exploited the system's symmetry to simplify the geometry to a single cylinder in a partly confined space. Since all cylinders are identical, concentration profiles expanding from Voronoi-type boundaries around each cylinder exhibit ideal symmetry with respect to that boundary. The simulation of a single Voronoi cell with 'no-flux' side planes and subsequent superposition of the result is hence an exact representation of the model. Within the diffusion domain approximation, we further approximated the outline of each Voronoi cell to be circular to enable the simulation in a cylindrical space, which, given that the original system features a hexagonal pattern, can be done in good approximation (See Figure S1). Herein, the surface area per cell is conserved leading to the following dependency on the above-defined parameters  $s$  and  $d$  and the radius  $r_d$  of the cylindrical diffusion domain:[32]

$$r_d^2 = \frac{1}{\pi} \sqrt{\frac{3}{2}} (d + s)^2 \quad (1)$$

In-depth software testing of the software's key functionality was done prior to and through results presented in a previous study,[23] and the rather minor modifications made in the context of this work are not expected to have any effect in this regard. Convergence was tested by dividing the key numerical parameters, *i.e.* the grid spacing at the electrode surface and the potential step width by a factor of ten and comparison of the results for the slowest and fastest scan rates with the data obtained for the parameters chosen in this work.

### 3. Results and Discussion

#### 3.1 Structure and Composition

The MWCNT textured glassy carbon electrodes that are obtained via the PECVD technique are vertically aligned on a GC surface. Due to a vapor–liquid–solid method tip-growth mechanism the nickel catalysts remain encapsulated at the tips of the MWCNTs resembling a nanoscopic bed of nails.[21] SEM images of such vertically aligned MWCNT textured glassy carbon surfaces are shown in Figure 1. In particular, Figure 1A-C show a GC surface textured with 500

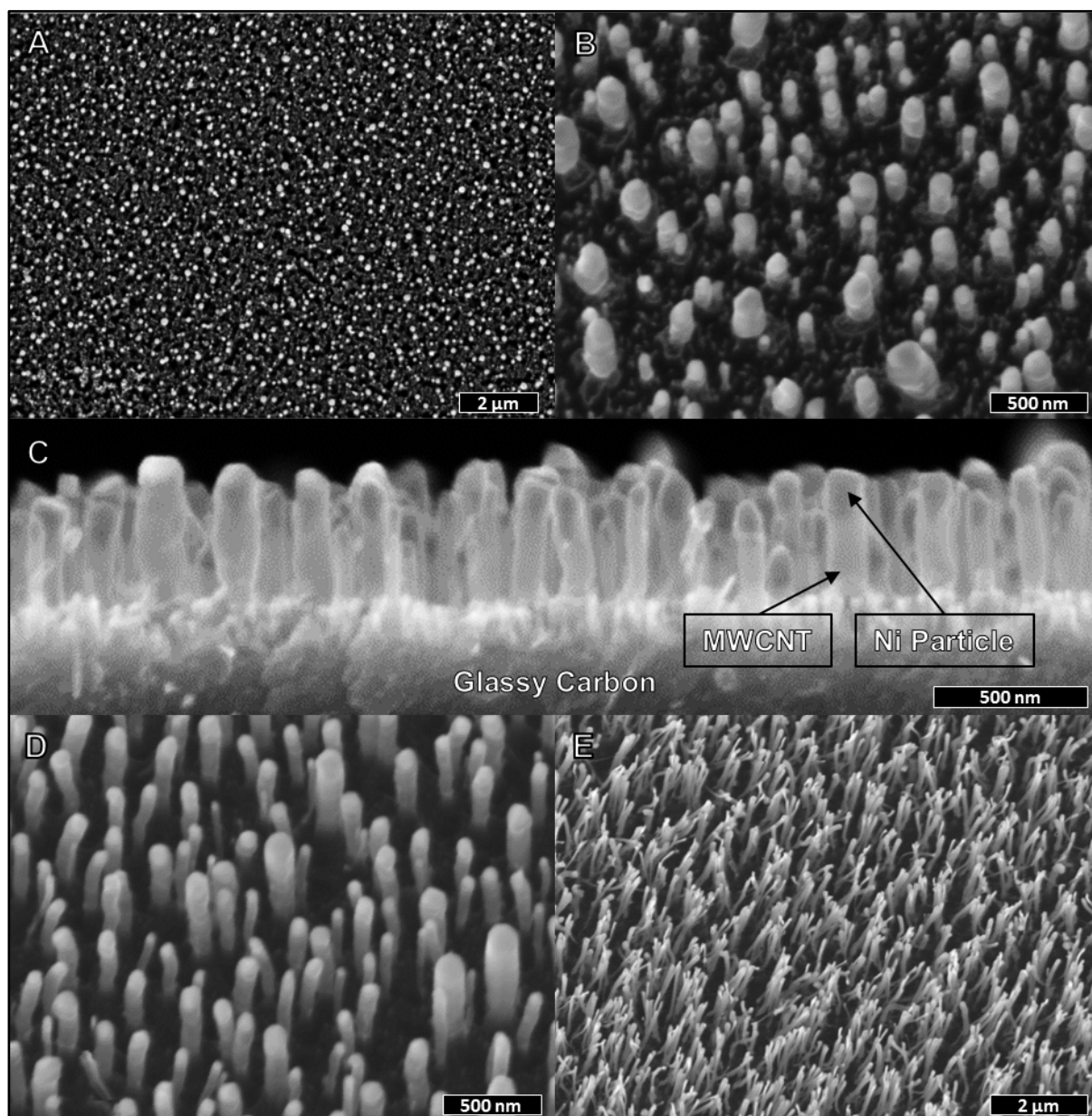


**Figure 1.** Scanning electron microscopy images of glassy carbon surfaces textured with vertically aligned MWCNTs. (A-C) show 500 nm long MWCNTs in (A) 0° - top, (B) 20° - tilted, and (C) 90° - cross-section view respectively. Further, GC textured with (D) 900 nm and (E) 3  $\mu$ m long MWCNTs in 20° tilted view are shown.

nm long MWCNTs in top, tilted and cross-section view respectively, and surfaces textured with substantially longer MWCNTs are shown in Figure 1D,E. The shades within the tips of the MWCNTs are the Ni catalyst particles, clearly visible in Figure 1C. An elemental analysis of the structure shows, that the Ni catalyst particles are located at the tips of the individual MWCNTs as can be seen in Figure S2 (supporting information). Here, EDX mapping signals of Ni are superimposed on an SEM image in Figure S2A (supporting information), whereas



Figure S2B,C show the Ni (cyan) and C (yellow) EDX signals respectively. To investigate the internal structure of the MWCNTs TEM investigations were performed. A TEM image of two MWCNTs of different size is shown in Figure S3A (supporting information), where the Ni catalyst particle is depicted with a strong contrast at the tip of the tubular carbon tube. It can be seen, that the MWCNTs widths are determined by the catalyst particle size that is encapsulated at their tips. Further, bamboo type compartments can be seen in the internal structure of the MWCNTs. The ultrastructure of the MWCNT is shown in Figure S3B showing graphitic planes. The inset shows an enlarged section of the sidewall from which a distance between planes of 0.34 nm typical for graphitic carbon could be deduced via FFT analysis.

### 3.2 Electrical Properties

To investigate the electrical properties of the carbon nanoarchitecture, current-voltage measurements are performed on individual vertically aligned MWCNTs and on their glassy carbon support utilizing a conductive AFM with an Au-tip in contact mode. A schematic illustration of the technique is shown in Figure S4A (supporting information). This geometry represents a two-electrode system, where the contacting electrodes are the Au-tip and the glassy carbon support respectively. In such a system, the specific contact resistance can be experimentally determined according to Equation 2:

$$R_C = \left\{ \frac{\partial V}{\partial I} \right\}_{V=0} \quad (2)$$

Thus, the total contact resistance  $R_{tot}$  of the system is represented by the inverse slope of the  $IV$ -curve in the vicinity of  $V = 0$ . The total measured contact resistance  $R_{tot}$  can then further be decomposes into a series circuit.[33] In the case of contacting individual MWCNTs the total contact resistance can be described by Equation 3:

$$R_{tot}^{CNT} \approx R_{tip} + R_{tip|CNT} + R_{CNT} + R_{CNT|GC} + R_{GC} \quad (3)$$

Here,  $R_{tip}$ ,  $R_{CNT}$  and  $R_{GC}$  are the intrinsic resistances of the gold coated tip, the MWCNTs and the glassy carbon support, and  $R_{tip|CNT}$  and  $R_{CNT|GC}$  are the contact resistances of the

tip/MWCNT and MWCNT/GC interfaces respectively. Similarly, contacting directly the GC support yields Equation 4:

$$R_{tot}^{GC} \approx R_{tip} + R_{tip|GC} + R_{GC} \quad (4)$$

Exemplary *IV*-curves for both cases are shown in Figure S4B. Here, the red data points correspond to the first case of MWCNTs described by Equation 3 and the blue data point correspond to the second case of the glassy carbon support described by Equation 4. The dashed lines are guides to the eye and show a linear trend typical for Ohmic contacts. The measured values for the total resistance of GC and several MWCNTs of two different lengths  $l$  (Samples S1 with  $l \approx 530$  nm and S2 with  $l \approx 720$  nm) are summarized in Table 1 and are in good agreement with values reported in similar systems.[5, 34, 35] The length of the MWCNTs is determined from SEM analysis based on the average MWCNT height of the arrays which is justified through the homogeneous growth and uniform length of the same. The deviation of total contact resistance between MWCNTs of similar length can be attributed to variation in MWCNT width, which is unequally dispersed and could not be extracted for individual measured MWCNTs via AFM techniques due to tip-sample convolution leading to profile broadening effects. Further, glassy carbon and MWCNTs are similar allotropes of carbon with a  $sp^2$ -hybridized structure. Therefore, a simplistic assumption, with  $R_{tip/GC} \approx R_{tip/CNT}$  then gives Equation 5:

$$R_{CNE} = R_{CNT} + R_{CNT|GC} \approx R_{tot}^{CNT} - R_{tot}^{GC} \quad (5)$$

The obtained values for the resistance of individual vertically aligned MWCNTs on glassy carbon of the proposed carbon nanoarchitecture electrode  $R_{CNE}$  summarized in Table 1.

**Table 1.** Contact resistance of vertically aligned MWCNTs on glassy carbon obtained by conductive atomic force microscopy.

	Glassy Carbon	S1 CNT 1	S1 CNT 2	S1 CNT 3	S2 CNT 1	S2 CNT 2	S2 CNT 3	S2 CNT 4
$I_{\text{mean}}$	-	530 nm	530 nm	530nm	720 nm	720 nm	720 nm	720 nm
$R_{\text{tot}}$	3.8 k $\Omega$	9.9 k $\Omega$	7.2 k $\Omega$	17.8 k $\Omega$	10.5 k $\Omega$	29.0 k $\Omega$	9.6 k $\Omega$	5.5 k $\Omega$
$R_{\text{CNE}}$	-	6.1 k $\Omega$	3.4 k $\Omega$	13.0 k $\Omega$	6.7 k $\Omega$	25.2 k $\Omega$	5.8 k $\Omega$	1.7 k $\Omega$

### 3.3 Electrochemical Response

The carbon nanoarchitecture with its promising structural and electronic properties renders the electrode feasible for use as a catalyst support in electrochemical catalysis. To obtain insights into the electrochemical processes that occur at the electrode surface, cyclic voltammetry studies are performed. The  $\text{Ru}(\text{NH}_3)_6^{3+/2+}$  couple was selected for study because of its generically fast electron transfer kinetics on many electrode material including carbon based electrodes so as to render negligible any possible contribution from the metal catalyst particles. Figure 2 shows cyclic voltammograms (CVs), where pristine GC as well as GC textured with MWCNTs that are 660 nm (short) and 4  $\mu\text{m}$  (long) in length were used as electrodes in a 1M KCl solution containing 1.0 mM  $\text{Ru}(\text{NH}_3)_6^{2+/3+}$  redox couple. CVs for a series of scan rates ranging from  $\nu=10 \text{ mVs}^{-1}$  to  $500 \text{ mVs}^{-1}$  were measured.

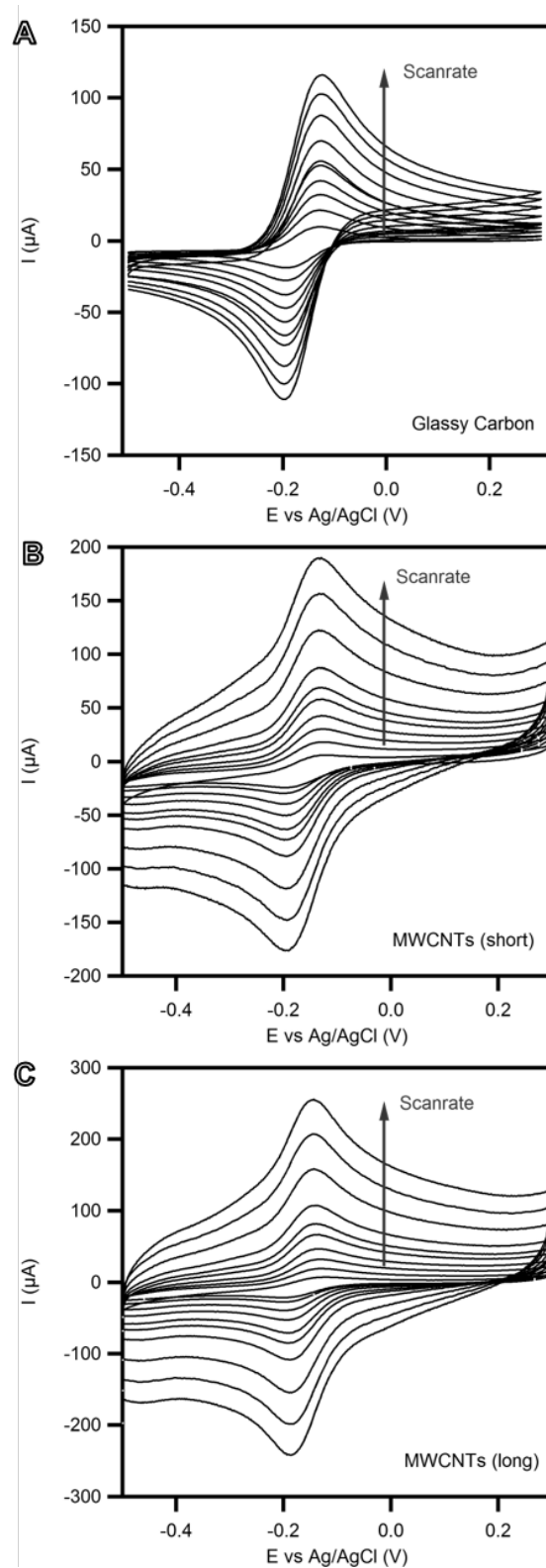


**Figure 2.** Cyclic voltammograms of (A) glassy carbon, and glassy carbon textured with (B) 660 nm, (C) 4  $\mu\text{m}$  MWCNTs in 1 mM  $\text{Ru}(\text{NH}_3)_6\text{Cl}_2$  in 1M KCl solution. Scan rates increase as 10, 25, 50, 80, 120, 150, 200, 300, 400, 500  $\text{mVs}^{-1}$  indicated by the arrows.

An obvious difference of all textured GC electrodes as compared to the pristine GC electrode is the observation of a large capacitive current. The CVs of the different electrodes in 1M KCl solution obtained for  $\nu = 120 \text{ mVs}^{-1}$  emphasize the increased capacitive behaviour of the textured electrodes (Figure 3). Whereas an interface capacitance equal to an ideal capacitor would lead to a rectangular CV, an increasing current is observed during the voltage sweep and the capacitance is, as expected, potential dependent. Clearly, the capacitance  $C_d$  of MWCNT textured electrodes is larger than for pristine GC electrodes and increased with MWCNT length. This is a result of the capacitive behaviour being dominated by double-layer capacitance which scales with surface area.

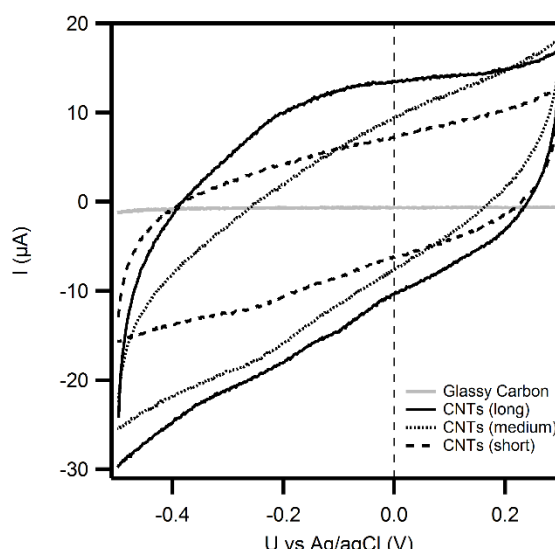


**Figure 3.** Cyclic voltammograms of pristine and glassy carbon textured with MWCNTs in 1M KCl solution. The scan rate is  $120 \text{ mVs}^{-1}$  for all CVs.

Further, conclusions on the electrode kinetics can be drawn from the cathodic and anodic peak heights and their separations. The system at hand is a Nernstian system at a macroelectrode where the mass transport follows Ficks's laws of diffusion.[27, 36] For planar macroelectrodes, linear diffusion can be assumed from bulk solution, which implies that the peak current  $I_p$  follows the Randles-Ševčík equation being proportional to  $\nu^{1/2}$ .[37] However, for porous films

with high surface area the linear diffusion model alone does not hold and the voltammetric response can be interpreted with aid of the voltammetric response of a thin-layer cell, where a small volume of solution is trapped in the thin porous film.[38] In such a thin-layer diffusion governed process, the CV peak current  $I_P$  is proportional to  $\nu$ , in contrast to  $\nu^{1/2}$  for processes governed by linear diffusion.[38] A log-log plot of  $I_P$  vs.  $\nu$  (Figure 4) reveals the expected  $I_P \sim \nu^{1/2}$  dependence for pristine GC deduced from the slope 0.5 exactly following Randles-Ševčík equation. In case of the short MWCNTs (blue) and more obvious for the long MWCNTs (green) it can be seen that the slope increases with scan rate. This can be attributed to a mixed thin-layer (slope 1) and linear diffusion (slope 0.5) response. For small  $\nu$  the textured electrodes behave like plane electrodes as only the linear diffusion from the bulk electrolyte to the geometrical area of the electrode is relevant. For large  $\nu$  the textured electrodes show a mixed response of linear diffusion to the MWCNT tips and the GC base between MWCNTs and a thin-layer response of MWCNT sidewalls to the electrolyte between MWCNTs.

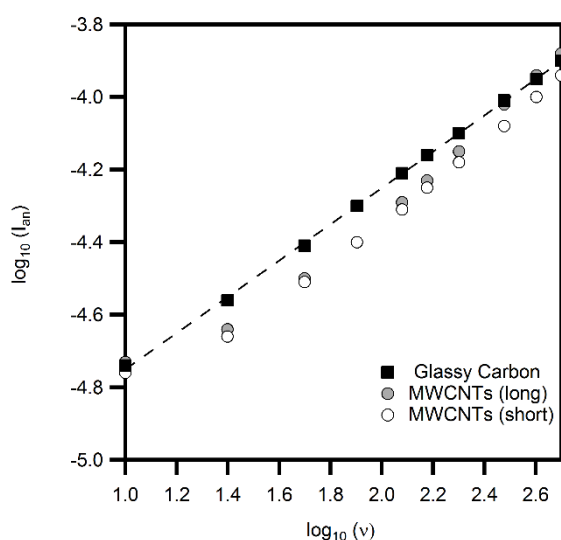


**Figure 4.** *log-log plot of the anodic peak current vs scan rate for MWCNT textured and pristine GC electrodes. The black dashed line is a linear fit with slope 0.5 in accordance to Randles-Ševčík equation.*

Additional information on the electrochemical processes can be inferred from the peak-to-peak separation  $\Delta E_{pp}$ . For linear diffusion at macroelectrodes  $\Delta E_{pp} = 2.218RT/F \approx 57$  mV (25°C) is

expected for a fast reversible single electron processes.[37] However, for ideal thin-layer diffusion  $\Delta E_{pp} = 0$ , as the diffusion time is very short and does not influence the voltammogram. The system then exhibits ideal symmetry with respect to the forward- and backward scan.[37–39] The peak-to-peak separation for the textured and pristine GC electrodes is shown in Figure 5A. Herein pristine GC shows an increase of  $\Delta E_{pp}$  of about 8 mV with  $\nu^{-1/2}$  over a range of nearly two orders of magnitude, which is a small deviation from the expected constant value and attributable to slight Ohmic drop. At textured GC electrodes  $\Delta E_{pp}$  decreases rapidly at first before it reaches a plateau which is indicative of an increased thin-layer contribution as  $\nu$  increases. These findings illustrate that textured GC electrodes behave similarly to planar electrodes for small  $\nu$  where the mass transport within the porous material takes place on a time scale that is by far exceeded by the time scale on which diffusion from the bulk occurs. In this case and the mass transport towards the electrode is dominated by the flux from the bulk and the contribution of material that is initially located within the porous layer can be neglected: The electroactive species between CNTs are consumed rapidly when the formal potential of the redox couple is approached and linear diffusion from bulk solution determines the CV response. For larger  $\nu$  the reaction of the electroactive species between the CNTs, which can be described as thin-layer diffusion, is increasingly significant for the CV response, which results in a decrease of  $\Delta E_{pp}$ . Similar systems have been investigated in recent years.[23, 39–41] For instance, drop casted CNTs formed random porous films on GC and showed a thin-layer response.[39, 40, 42] These were described with a theoretical model based on vertically aligned pillars.[40] In the model considered here, a single cylinder on an inactive flat surface is considered as an electrode, which is centred within a larger cylinder that represents the diffusion domain.[23] The system can then be described through Fick's second law in cylindrical coordinates

$$\frac{1}{D} \frac{\partial c}{\partial t} = \frac{\partial^2 c}{\partial z^2} + \frac{1}{r} \frac{\partial c}{\partial r} + \frac{\partial^2 c}{\partial r^2} \quad (6)$$

with concentration  $c$ , time  $t$  and coordinates  $r$  and  $z$ . The equation is then solved numerically subject to boundary conditions that result from the geometry of the system.[23] The theoretical model correlates well to the MWCNT textured GC electrode system presented here. To enable a qualitative comparison between simulation and experiment, the geometrical input parameters for the simulations were approximated from SEM images from which the mean MWCNT diameter and MWCNT density was deduced. The extracted  $\Delta E_{pp}$  from simulation and experiment of GC electrodes textured with long MWCNTs is shown in Figure 5B and shows a clear agreement of the trend so that the mass diffusion process is confirmed qualitatively.

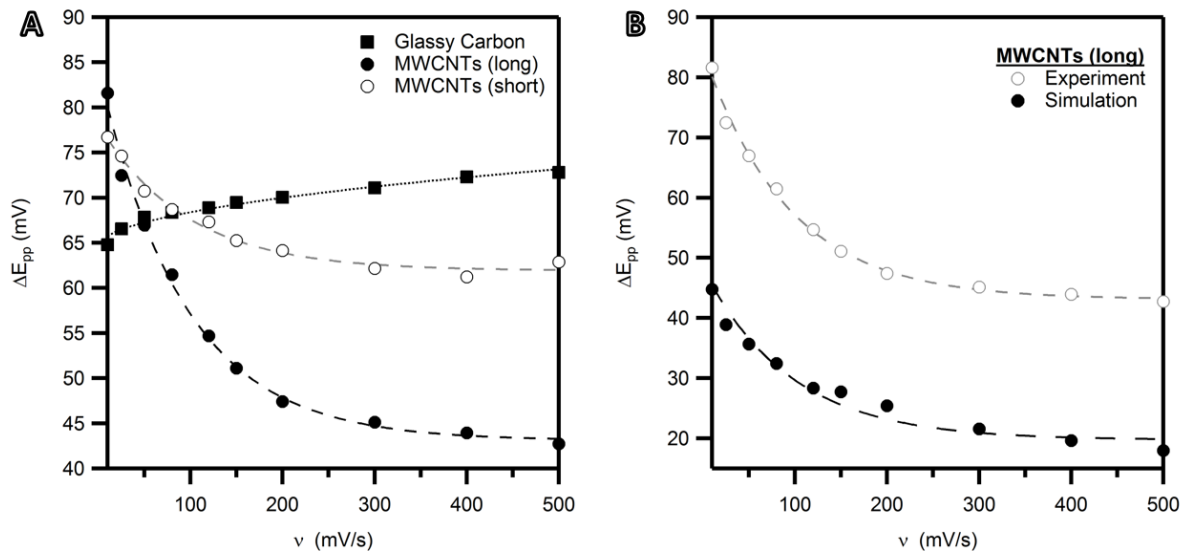


**Figure 5.** (A)  $\Delta E_{pp}$  vs.  $\nu$  for the same samples (B) Simulated and experimental  $\Delta E_{pp}$  vs.  $\nu$  overlaid for a GC electrode textured with long MWCNTs with clearly similar trend. Simulations herein assume Nernstian kinetics.

#### 4. Conclusions

In conclusion, we demonstrated that vertically aligned spaced out MWCNTs can directly be grown on glassy carbon, exhibit a good electrical contact, and can be used as a nanostructured macroelectrode. It was shown, that the capacitance of these electrodes increases with the length of the grown nanotubes and that the electrode morphology leads to a change in the mass



transport characteristics exhibiting a mixed linear- and thin-layer diffusion response. The findings are qualitatively supported through simulations. This carbon electrode with nanoscale architectures is an ideal candidate to design wired composites where this electrode is the backbone with good intrinsic electrical conductivity and may be used to support electrochemically active materials. Our results provide a deeper understanding of the electrochemical response of vertically aligned arrays of one dimensional nanomaterials and show, that their voltammetric response is influenced by morphology dependent diffusion properties strongly deviating from planar macro electrodes.

### **Acknowledgements**

The authors thank U Bloeck and K Ellmer from Helmholtz-Zentrum Berlin for access to equipment. The research leading to these results has received partial funding from the Guangdong Innovative and Entrepreneurial Team Program titled “Plasmonic Nanomaterials and Quantum Dots for Light Management in Optoelectronic Devices” (No.2016ZT06C517) and partial funding from the European Research Council under the European Union's Seventh Framework Programme (FP/2007-2013) / ERC Grand Agreement no. [320403].

## References

- [1] McCreery RL. Advanced carbon electrode materials for molecular electrochemistry. *Chemical reviews* 2008;108(7):2646–87.
- [2] Lipkowski J, Bartlett PN, Alkire RC (eds.). *Electrochemistry of carbon electrodes*. Weinheim, Germany: Wiley-VCH; 2015.
- [3] Valcarcel M, Cardenas S, Simonet BM. Role of carbon nanotubes in analytical science. *Analytical chemistry* 2007;79(13):4788–97.
- [4] Wildgoose GG, Banks CE, Leventis HC, Compton RG. Chemically Modified Carbon Nanotubes for Use in Electroanalysis. *Microchim Acta*;152(3-4):187–214.
- [5] Ando Y, Zhao X, Shimoyama H, Sakai G, Kaneto K. Physical properties of multiwalled carbon nanotubes. *International Journal of Inorganic Materials* 1999;1(1):77–82.
- [6] Jang JW, Lee DK, Lee CE, Lee TJ, Lee CJ, Noh SJ. Metallic conductivity in bamboo-shaped multiwalled carbon nanotubes. *Solid State Communications* 2002;122(11):619–22.
- [7] Li HJ, Lu WG, Li JJ, Bai XD, Gu CZ. Multichannel ballistic transport in multiwall carbon nanotubes. *Physical review letters* 2005;95(8):86601.
- [8] Serp P. Carbon nanotubes and nanofibers in catalysis. *Applied Catalysis A: General* 2003;253(2):337–58.
- [9] Gooding JJ. Nanostructuring electrodes with carbon nanotubes: A review on electrochemistry and applications for sensing. *Electrochimica Acta* 2005;50(15):3049–60.
- [10] Wang J. Carbon-Nanotube Based Electrochemical Biosensors: A Review. *Electroanalysis* 2005;17(1):7–14.
- [11] Liu G, Wang S, Liu J, Song D. An electrochemical immunosensor based on chemical assembly of vertically aligned carbon nanotubes on carbon substrates for direct detection of the pesticide endosulfan in environmental water. *Analytical chemistry* 2012;84(9):3921–8.
- [12] Obreja VV. On the performance of supercapacitors with electrodes based on carbon nanotubes and carbon activated material—A review. *Physica E: Low-dimensional Systems and Nanostructures* 2008;40(7):2596–605.
- [13] Zhang LL, Zhao XS. Carbon-based materials as supercapacitor electrodes. *Chemical Society reviews* 2009;38(9):2520–31.
- [14] Pumera M. The electrochemistry of carbon nanotubes: fundamentals and applications. *Chemistry (Weinheim an der Bergstrasse, Germany)* 2009;15(20):4970–8.
- [15] Dumitrescu I, Unwin PR, Macpherson JV. Electrochemistry at carbon nanotubes: perspective and issues. *Chemical communications (Cambridge, England)* 2009(45):6886–901.
- [16] Wang Y, Du G, Zhu L, Liu H, Wong C, Wang J. Aligned open-ended carbon nanotube membranes for direct electrochemistry applications. *Sensors and Actuators B: Chemical* 2012;174:570–6.
- [17] Park S, Park D, Yang C, Kim K, Kwak J, So H et al. Vertically aligned carbon nanotube electrodes directly grown on a glassy carbon electrode. *ACS nano* 2011;5(9):7061–8.
- [18] Kim KJ, Yu WR, Youk JH, Lee J. Factors governing the growth mode of carbon nanotubes on carbon-based substrates. *Physical chemistry chemical physics PCCP* 2012;14(40):14041–8.
- [19] Li W, Wang D, Yang S, Wen J, Ren Z. Controlled growth of carbon nanotubes on graphite foil by chemical vapor deposition. *Chemical Physics Letters* 2001;335(3-4):141–9.
- [20] Chen P, Fryling MA, McCreery RL. Electron Transfer Kinetics at Modified Carbon Electrode Surfaces: The Role of Specific Surface Sites. *Anal. Chem.* 2002;67(18):3115–22.
- [21] Ren Z, Lan Y, Wang Y. *Aligned carbon nanotubes: Physics, concepts, fabrication and devices*. Berlin, New York: Springer; 2013.
- [22] Huang ZP, Carnahan DL, Rybczynski J, Giersig M, Sennett M, Wang DZ et al. Growth of large periodic arrays of carbon nanotubes. *Appl. Phys. Lett.* 2003;82(3):460.

- [23] Ban Z, Kätelhön E, Compton RG. Voltammetry of porous layers: Staircase vs analog voltammetry. *Journal of Electroanalytical Chemistry* 2016;776:25–33.
- [24] Henstridge MC, Dickinson EJF, Compton RG. Mass transport to and within porous electrodes. Linear sweep voltammetry and the effects of pore size: The prediction of double peaks for a single electrode process. *Russ J Electrochem* 2012;48(6):629–35.
- [25] Streeter I, Xiao L, Wildgoose GG, Compton RG. Gold Nanoparticle-Modified Carbon Nanotubes-Modified Electrodes. Using Voltammetry to Measure the Total Length of the Nanotubes. *J. Phys. Chem. C* 2008;112(6):1933–7.
- [26] Godino N, Borrisse X, Munoz FX, del Campo FJ, Compton RG. Mass Transport to Nanoelectrode Arrays and Limitations of the Diffusion Domain Approach: Theory and Experiment. *J. Phys. Chem. C* 2009;113(25):11119–25.
- [27] Wang Y, Limon-Petersen JG, Compton RG. Measurement of the diffusion coefficients of  $[\text{Ru}(\text{NH}_3)_6]^{3+}$  and  $[\text{Ru}(\text{NH}_3)_6]^{2+}$  in aqueous solution using microelectrode double potential step chronoamperometry. *Journal of Electroanalytical Chemistry* 2011;652(1-2):13–7.
- [28] Scharifker BR. Diffusion to ensembles of microelectrodes. *Journal of Electroanalytical Chemistry and Interfacial Electrochemistry* 1988;240(1-2):61–76.
- [29] Davies TJ, Banks CE, Compton RG. Voltammetry at spatially heterogeneous electrodes. *J Solid State Electrochem* 2005;9(12):797–808.
- [30] Sliusarenko O, Oleinick A, Svir I, Amatore C. Validating a Central Approximation in Theories of Regular Electrode Electrochemical Arrays of Various Common Geometries. *Electroanalysis* 2015;27(4):980–91.
- [31] Brookes BA, Davies TJ, Fisher AC, Evans RG, Wilkins SJ, Yunus K et al. Computational and Experimental Study of the Cyclic Voltammetry Response of Partially Blocked Electrodes. Part 1. Nonoverlapping, Uniformly Distributed Blocking Systems. *J. Phys. Chem. B* 2003;107(7):1616–27.
- [32] Compton RG, Banks CE. *Understanding voltammetry*. 2<sup>nd</sup> ed. London: Imperial College Press; 2011.
- [33] Alvarez J, Ngo I, Gueunier-Farret M, Kleider J, Yu L, Cabarrocas PR et al. Conductive-probe atomic force microscopy characterization of silicon nanowire. *Nanoscale Research Letters* 2011;6(1):1.
- [34] Ghanem TK, Williams ED, Fuhrer MS. Characterization of the electrical contact between a conductive atomic force microscope cantilever and a carbon nanotube. *J. Appl. Phys.* 2011;110(5):54305.
- [35] Toader M, Fiedler H, Hermann S, Schulz SE, Gessner T, Hietschold M. Conductive AFM for CNT characterization. *Nanoscale Research Letters* 2013;8(1):24.
- [36] Limon-Petersen JG, Han JT, Rees NV, Dickinson EJF, Streeter I, Compton RG. Quantitative Voltammetry in Weakly Supported Media. Chronoamperometric Studies on Diverse One Electron Redox Couples Containing Various Charged Species: Dissecting Diffusional and Migrational Contributions and Assessing the Breakdown of Electroneutrality. *J. Phys. Chem. C* 2010;114(5):2227–36.
- [37] Bard AJ, Faulkner LR. *Electrochemical methods: Fundamentals and applications*. 2<sup>nd</sup> ed. New York: Wiley; 2001.
- [38] Barnes EO, Chen X, Li P, Compton RG. Voltammetry at porous electrodes: A theoretical study. *Journal of Electroanalytical Chemistry* 2014;720-721:92–100.
- [39] Streeter I, Wildgoose GG, Shao L, Compton RG. Cyclic voltammetry on electrode surfaces covered with porous layers: An analysis of electron transfer kinetics at single-walled carbon nanotube modified electrodes. *Sensors and Actuators B: Chemical* 2008;133(2):462–6.
- [40] Henstridge MC, Dickinson EJ, Aslanoglu M, Batchelor-McAuley C, Compton RG. Voltammetric selectivity conferred by the modification of electrodes using conductive porous layers or films:

The oxidation of dopamine on glassy carbon electrodes modified with multiwalled carbon nanotubes. *Sensors and Actuators B: Chemical* 2010;145(1):417–27.

[41] Prehn R, Abad L, Sánchez-Molas D, Duch M, Sabaté N, del Campo FJ et al. Microfabrication and characterization of cylinder micropillar array electrodes. *Journal of Electroanalytical Chemistry* 2011;662(2):361–70.

[42] Sims MJ, Rees NV, Dickinson EJ, Compton RG. Effects of thin-layer diffusion in the electrochemical detection of nicotine on basal plane pyrolytic graphite (BPPG) electrodes modified with layers of multi-walled carbon nanotubes (MWCNT-BPPG). *Sensors and Actuators B: Chemical* 2010;144(1):153–8.

## Supplemental Information

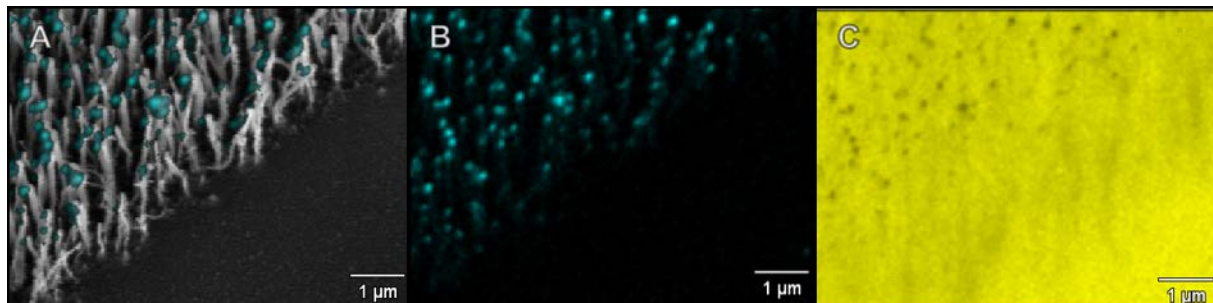


**Figure S1.** Elemental analysis of MWCNT textured glassy carbon electrodes. (A) SEM image of a typical electrode in 20° tilted perspective with the Ni EDX mapping signal superposed in cyan. The Ni and C signals are explicitly shown in (B) and (C) respectively. Clearly, the Ni signals are obtained from the tips of the MWCNTs.

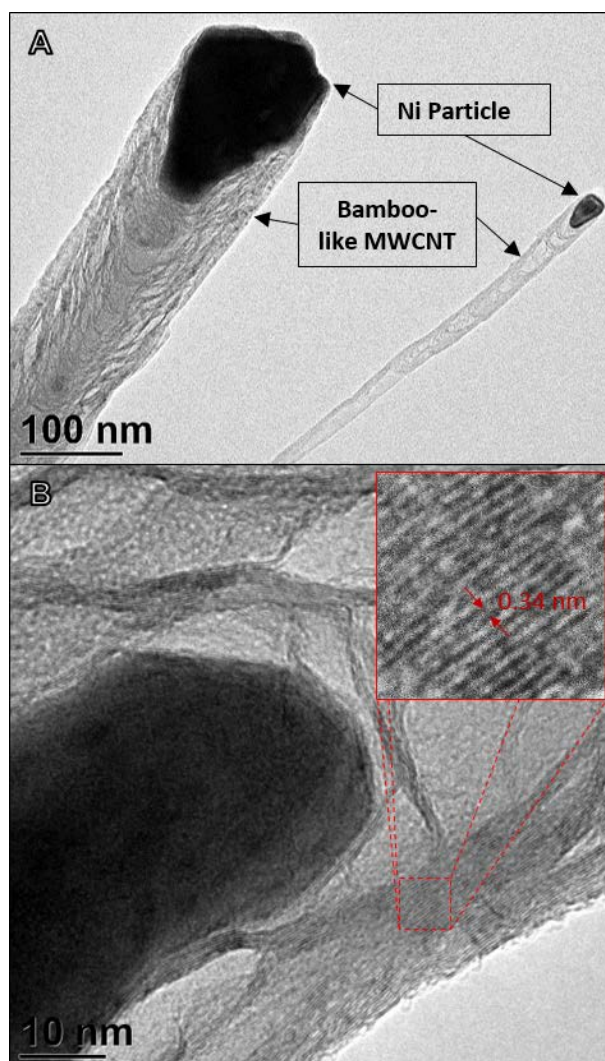


**Figure S2.** (A) Transmission electron microscopy images of MWCNTs grown on glassy carbon surfaces. The MWCNTs are bamboo-like with Ni catalyst particles encapsulated at their tips. (B) Ultrastructure of a MWCNT. The red inset shows an enlargement of the sidewall with 0.34 nm distance between the individual graphitic planes.

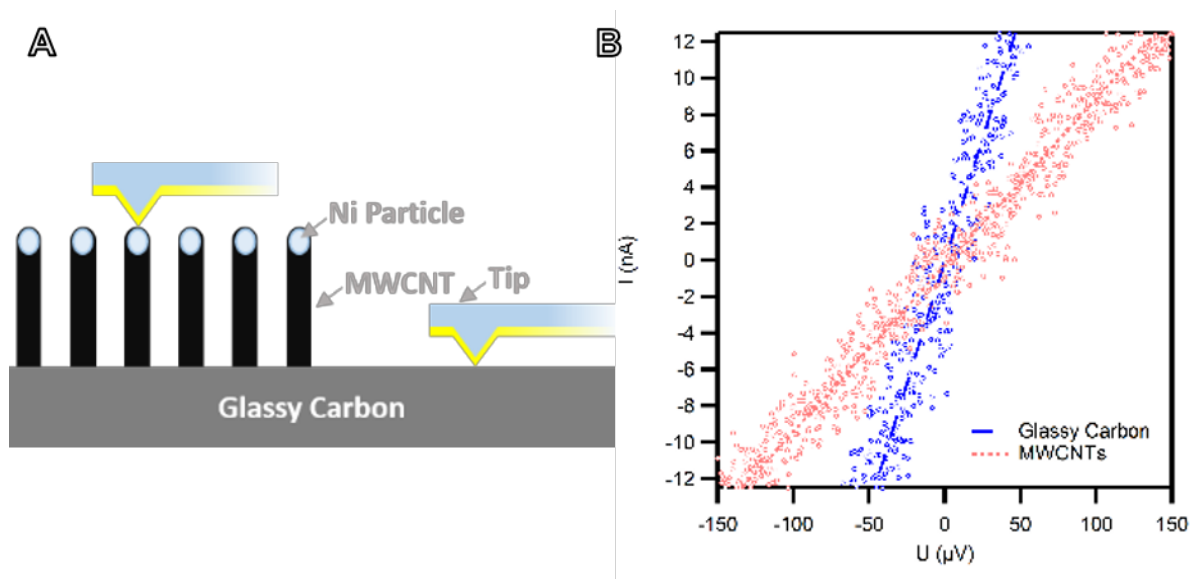


**Figure S3.** Contact resistance measurements of vertically aligned MWCNTs on glassy carbon via conductive atomic force microscopy. (A) Schematic illustration of the technique. A Au coated AFM tip is used to collect IV-curves of individual vertically aligned MWCNTs. (B) IV-curves of MWCNT (red) and glassy carbon (blue). The dashed lines are a guide to the eye.

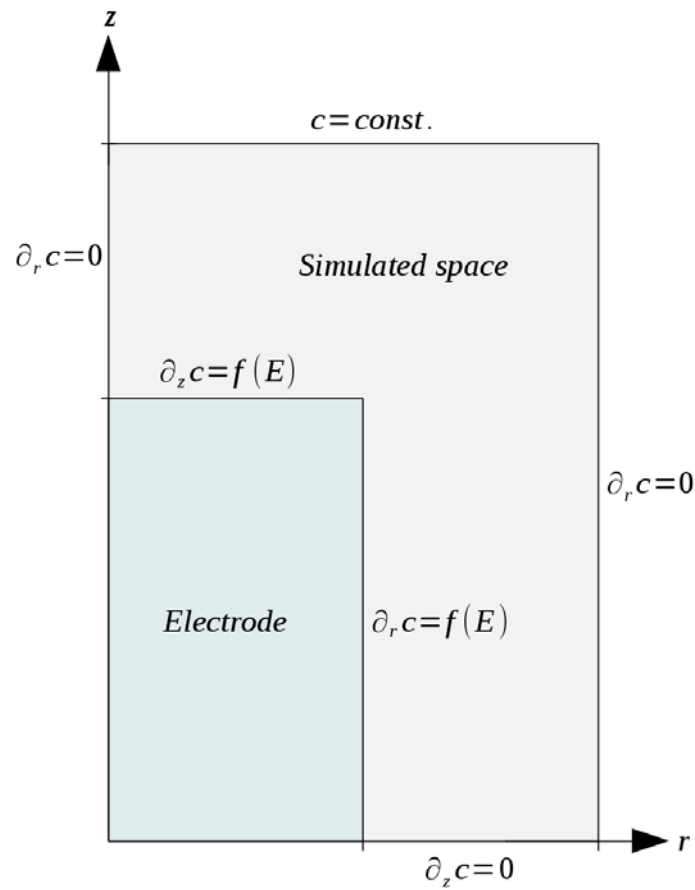


**Figure S4.** Single Voronoi cell with 'no-flux' side planes. The outline of each Voronoi cell is approximated to be circular to enable the simulation in a cylindrical space.